IR Spectroscopy of b(4) Fragment Ions of Protonated Pentapeptides in the X–H (X = C, N, O) Region

ARTICLE *in* THE JOURNAL OF PHYSICAL CHEMISTRY A · FEBRUARY 2013

Impact Factor: 2.69 · DOI: 10.1021/jp400634t · Source: PubMed

5 AUTHORS, INCLUDING:

Maximiliano Rossa
National University of Cordoba, Argentina
10 PUBLICATIONS **50** CITATIONS
SEE PROFILE

Oscar Hernandez
Université Paris-Sud 11
7 PUBLICATIONS **28** CITATIONS
SEE PROFILE

Philippe Maître
Université Paris-Sud 11
140 PUBLICATIONS **3,548** CITATIONS
SEE PROFILE

THE JOURNAL OF PHYSICAL CHEMISTRY A

Article

pubs.acs.org/JPCA

IR Spectroscopy of b_4 Fragment Ions of Protonated Pentapeptides in the X–H (X = C, N, O) Region

Sylvère Durand,[†] Maximiliano Rossa,[†] Oscar Hernandez,[†] Béla Paizs,*[,§,‡] and Philippe Maître*[,†]

[†]Laboratoire de Chimie Physique, Université Paris Sud, UMR8000 CNRS, Faculté des Sciences, Bât. 350, 91405 Orsay Cedex, France

[‡]Computational Proteomics Group, German Cancer Research Center, Im Neuenheimer Feld 580, 69120 Heidelberg, Germany

[§]School of Chemistry, Bangor University, Bangor, Gwynedd LL57 2UW, U.K.

Supporting Information

ABSTRACT: The structure of peptide fragments was studied using "action" IR spectroscopy. We report on room temperature IR spectra of b_4 fragments of protonated GGGGG, AAAAA, and YGGFL in the X–H (X = C, N, O) stretching region. Experiments were performed with a tandem mass spectrometer combined with a table top tunable laser, and the multiple photon absorption process was assisted using an auxiliary high-power CO_2 laser. These experiments provided well-resolved spectra with relatively narrow peaks in the X–H (X = C, N, O) stretching region for the b_4 fragments of protonated GGGGG, AAAAA, and YGGFL. The 3200–3700 cm^{-1} range of the first two of these spectra are rather similar, and the corresponding peaks can be assigned on the basis of the classical b ion structure that has a linear backbone terminated by the oxazolone ring at the C-terminus and ionizing proton residing on the oxazolone ring nitrogen. The spectrum of the b_4 of YGGFL, on the other hand, is different from the two others and is characterized by a band observed near 3238 cm^{-1}. Similar band positions have recently been reported for one of the four isomers of the b_4 of YGGFL studied using double resonance IR/UV technique. As proposed in this study, the IR spectrum of this ion at room temperature can also be assigned to a linear N-terminal amine protonated oxazolone structure. However, an alternative assignment could be proposed because our room temperature IR spectrum of the b_4 of YGGFL nicely matches with the predicted IR absorption spectrum of a macrocyclic structure. Because not all experimental IR features are unambiguously assigned on the basis of the available literature structures, further theoretical studies will be required to fully exploit the benefits offered by IR spectroscopy in the X–H (X = C, N, O) stretching region.

INTRODUCTION

Protein identification in the rapidly exploding field of proteomics is mainly based on sequencing of proteolytic peptides[1] using tandem mass spectrometry (MS/MS). In these experiments protonated peptides are activated by collisions with inert gases to induce dissociation (collision induced dissociation, CID) and the information encoded in the resulting backbone b, a, and y fragments,[2,3] is used for sequencing. The related data processing is mostly achieved by various bioinformatics tools,[4] which generate and evaluate a spectrum-to-sequence matches. The crucial step in this process is creation of theoretical (*in silico*) dissociation patterns (theoretical spectra) for candidate sequences based on fragmentation models[5] that summarize our understanding of how protonated peptides fragment in mass spectrometers. It is generally believed[5] that the currently used fragmentation models are oversimplified and more advanced strategies need to be developed to predict fragmentation patterns that better approximate the experimentally observed CID spectra. Therefore, the past decade has seen an explosion[5] of experimental and theoretical work devoted to deepening our understanding of gas-phase peptide fragmentation chemistry.

Recently, IR "action" spectroscopy[6-13] making use of IR multiple photon dissociation (IRMPD) has been successfully adapted to determine the structures of various peptide fragments. In these experiments the target ions isolated in trapping mass spectrometers are irradiated by tunable lasers to induce dissociation and the fragmentation yield is monitored to generate IR "action" spectra. To fragment protonated peptides and their fragments, the laser applied needs to be able to break covalent bonds. In this respect, highly intense and pulsed infrared free-electron lasers (FELs)[14,15] probing the "fingerprint" IR range have been shown to be particularly well suited and such studies provided invaluable information on b and a fragments of peptide ions significantly deepening our understanding of the related fragmentation chemistries. In their classical papers[16,17] published more than a decade ago Harrison and co-workers proposed that b ions have a linear backbone that is terminated by the five-membered oxazolone ring. Though this hypothesis rationalized numerous fragmentation observations,[5] the first direct demonstration of the oxazolone structure arose in an IR study of the b_4 ion of YGGFL.[6] This was followed by a number of studies on smaller b_n ions,[8,9,13] most of which confirmed the proposed oxazolone structure. In

Received: January 19, 2013
Revised: February 22, 2013
Published: February 25, 2013

dx.doi.org/10.1021/jp400634t | J. Phys. Chem. A 2013, 117, 2508–2516

the case of histidine-containing b_2 ions, however, a mixture of oxazolone and diketopiperazine structures has been evidenced by IRMPD spectroscopy.[18] Recently, it was suggested that the oxazolone-terminated linear isomers of middle-sized b_n ions undergo head-to-tail cyclization[19] forming macrocyclic isomers. This chemistry can be deteriorating for sequencing because it can lead to scrambling[20] of the original amino acid sequence. Again, IR spectroscopy provided the first direct evidence for the existence of a macrocyclic b ion.[10] More recently, IR spectroscopy demonstrated that similar macrocyclization[7,11] and subsequent sequence rearrangement[12] can also occur with a_n fragment ions. Even this short and rather incomplete list indicates the enormous advances provided by "action" IR spectroscopy in deducing structures of peptide fragments.

Extending the IR range to cover the X−H (X = C, O, N) stretching region is particularly useful because it may also provide IR signatures of specific structural motifs associated with hydrogen-bonding. IR spectroscopy in this spectral range has been performed on gas-phase amino-acids[21−23] and peptides,[24,25] and more recently on electrosprayed peptides[26,27] using double resonance IR/UV or the messenger techniques,[28] recently coupled with a double resonance IR/IR approach. Although the double resonance IR/UV techniques are restricted to species containing an aromatic chromophore, they present advantages as they are not only mass-selective but also isomer selective. Of particular importance for the present study is the recent IR/UV investigation of the b_2, b_3, b_4, and also a_4 ions[27] of protonated YGGFL by Rizzo and co-workers. High-resolution IR spectra of various conformers of these ions have been recorded and a structural assignment has been proposed. The vibrational analysis and assignment was supported by nitrogen-15 isotopic substitution of individual amino-acid residues and assisted by DFT calculations. All b_n (b_2, b_3, and b_4) ions were found to have an oxazolone structure with linear backbone protonated on the N-terminal amino group. The recently proposed rearranged amine−amide structure of the a_4 ion[12] formed by macrocyclization and subsequent alternative ring-opening was clearly confirmed by the IR/UV signatures. On the other hand, the IR/UV experiment suggests that no macrocyclic or scrambled linear b_4 ion is formed whereas the former could be observed to some extent in a previous FEL IRMPD study.[7]

Gas-phase peptide chemistry would no doubt hugely benefit from widespread access to IR studies on various peptide fragment ions. Because of limited access to high-end IR FEL lasers, it is desirable to develop strategies that are based on simple combinations of table-top IR lasers with commercial tandem mass spectrometers. The principle motivation of this work was to perform IR spectroscopy of room temperature middle-sized b_n fragments in the X−H (X = C, N, O) stretching region. In these experiments the table-top OPO/OPA is coupled to a high-power CO_2 laser to improve sensitivity of "action" IR spectroscopy. With this experimental setup, the b_4 fragments of protonated GGGGG, AAAAA, i.e., containing no aromatic chromophore were studied, as well as the b_4 fragments of protonated YGGFL.

METHODS

The IR spectra were recorded using a 7 T Fourier transform ion cyclotron resonance (FT-ICR) tandem mass spectrometer (Bruker Apex Qe) coupled with an optical parametric oscillator/amplifier (OPO/OPA from LaserVision) laser system.[29] This laser system is pumped by an Innolas Spitlight 600 nonseeded Nd:YAG (1064 nm, 550 mJ/pulse, bandwidth ∼1 cm^{-1}) laser running at 25 Hz and delivering pulses of 4−6 ns duration. The typical output energy of the OPO/OPA was 12−13 mJ/pulse at 3600 cm^{-1} with a 3−4 cm^{-1} (fwhm) bandwidth. Whereas weakly bound ions such as hydrated ions can be efficiently fragmented upon resonant IR activation,[30,31] the IR induced fragmentation process of strongly bound ions can be efficiently assisted using an auxiliary CO_2 laser.[29,32] As described elsewhere,[32] a few milliseconds long CO_2 pulse follows each OPO/OPA pulse, delayed by ∼1 μs. It should be noted that combination of a tunable IR laser with a line tunable CO_2 laser, which was first proposed by Y. T. Lee and co-workers,[33] has also been used by the Eyler group,[34] and more recently by Rizzo and co-workers[35] to assist double resonance UV/IR spectroscopy in the case of large protonated peptides.

GGGGG, AAAAA, and YGGFL [American Peptide Co. (Sunnyvale, CA, USA)] were dissolved in CH_3OH:H_2O = 1:1 with 2% acetic acid in a concentration range of ca. 50−80 mmol·L^{-1} and sprayed with conventional electrospray (ESI) conditions. The ESI-formed protonated peptides were mass selected and then allowed to collide with argon within the pressurized hexapole accumulation trap of the quadrupole−hexapole (Qh) interface of the 7T hybrid FT-ICR mass spectrometer. Ions were then pulse-driven into the ICR cell, where b_4 ions were mass-selected and then subjected to IR irradiation. Using the combination of OPO/OPA and CO_2 lasers, the irradiation time was set to 1 s.

Upon resonant vibrational excitation, dissociation of the b_4 ions was monitored via the a_4 and, in the cases of GGGGG and AAAAA, the b_4^0 peaks. At each laser wavelength, the abundances of the precursor and photofragment ions were derived from the mass spectrum recorded by Fourier transform of the average of five time-domain transients. The IRMPD spectrum is obtained by plotting the photodissociation efficiency $-\ln(I_{parent}/(I_{parent}+\Sigma I_{fragment}))$ as a function of the laser wavenumber.

The theoretical IR spectra were determined using harmonic frequencies computed at the B3LYP/6-31+G(d,p) level and scaled by the same factor value of 0.955 as used for b_2 ions.[29] The theoretical structures were taken from scans reported in the literature except for the macrocyclic isomer with the GGGG sequence, which was determined using the strategy described in refs 7 and 12. The Gaussian set of programs[36] was used for all ab initio and DFT calculations and zero-point energy (ZPE) corrected total and free energies were calculated using harmonic vibrational frequencies.

RESULTS AND DISCUSSION

The IR spectra of the three investigated b_4 ions are given in Figure 1. As can be seen, the IR spectrum of the YGGF b_4 fragment is clearly different from the two others. The IR spectra of the GGGG and AAAA b_4 ions (Figure 1a,b, respectively) are rather similar, featuring two major bands with a similar splitting (120−140 cm^{-1}). In the GGGG case a rather symmetric band is observed at ∼3358 cm^{-1}, and an asymmetric band is observed at higher photon energy (∼3478 cm^{-1}) with a shoulder on its red side. The corresponding ∼3464 cm^{-1} band for the AAAA b_4 ion also has a shoulder on its red side. The band observed at lower energy, with a maximum at ∼3322 cm^{-1}, is asymmetric with a shoulder on its blue side at ∼3355 cm^{-1}.

The IR spectrum of the YGGF b_4 ion (Figure 1c) is more structured than the those of the GGGG and AAAA b_4 ions

dx.doi.org/10.1021/jp400634t | J. Phys. Chem. A 2013, 117, 2508−2516

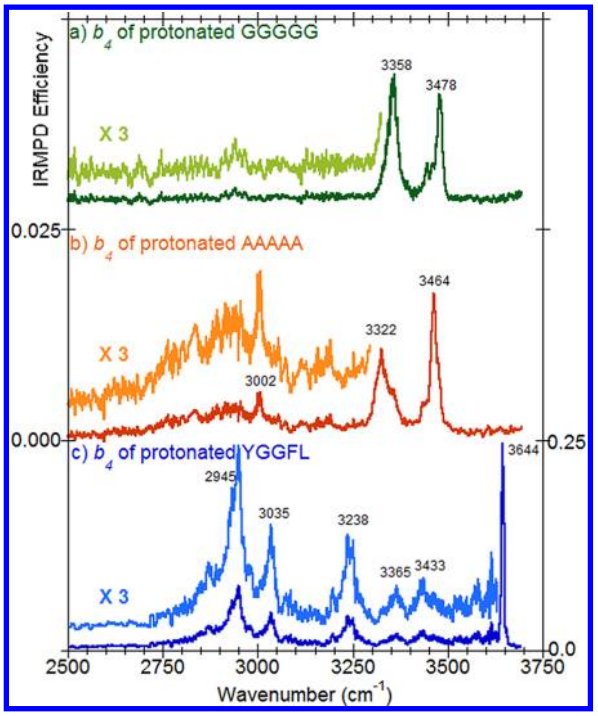

Figure 1. Experimental infrared spectra of the b_4 ion of protonated (a) GGGGG, (b) AAAAA, and (c) YGGFL.

(Figure 1a,b, respectively). The sharp (fwhm = 10 cm^{-1}) band centered at 3644 cm^{-1} can be assigned to the tyrosine OH stretching mode.[27,29] Two weak bands are observed in the spectral range where the GGGG and AAAA b_4 ions display two intense features; one broad band with a maximum at ~3433 cm^{-1}, and a better defined band at ~3365 cm^{-1} (Figure 1c). The fourth distinct band of the YGGF b_4 ion has its maximum at 3238 cm^{-1}; this is characteristic of the YGGF b_4 fragment because neither the GGGG (Figure 1a) nor the AAAA (Figure 1b) spectrum displays any IRMPD signal here.

In the lower energy region of the GGGG and AAAA spectra, a broad yet structured band extending from ~2700 to ~3100 cm^{-1} can be observed. The IR spectrum in this range could be interpreted as a convolution of one broad band and sharper bands. In the AAAA case (Figure 1b), one sharp maximum can be clearly observed at ~3002 cm^{-1}. The IRMPD signal is less intense in the case of the b_4 ions of protonated GGGGG, but yet a band centered at ~2950 cm^{-1} can be distinguished. In the YGGF case two sharp features are present with maxima at ~2945 and ~3035 cm^{-1}.

Recent theoretical and FEL-IR studies[6,7,19,20] indicate that one needs to consider three major structures for peptide b_4 ions (Scheme 1). Protonated peptides fragment[5] to form b ions with a linear backbone that is terminated by the five-membered oxazolone ring. This structure features two energetically favored protonation sites; the oxazolone ring nitrogen (structure A in Scheme 1A) and the N-terminal amino group (structure B in Scheme 1B). The initially formed linear structure can undergo head-to-tail cyclization[19,20] forming a macrocyclic isomer (structure C in Scheme 1C); the preferential protonation sites of this structure are the amide carbonyl oxygens.

Theoretical IR spectra for a variety of conformers of the three major structures of the studied b_4 ions have been calculated in the present work. The geometries of the A and B structures of the GGGG b_4 ions (Figure S1, Supporting

Scheme 1. Ring-Protonated Oxazolone (A), N-Terminal Amino Protonated Oxazolone (B), and Macrocyclic (C) Isomers of b_4 Ions

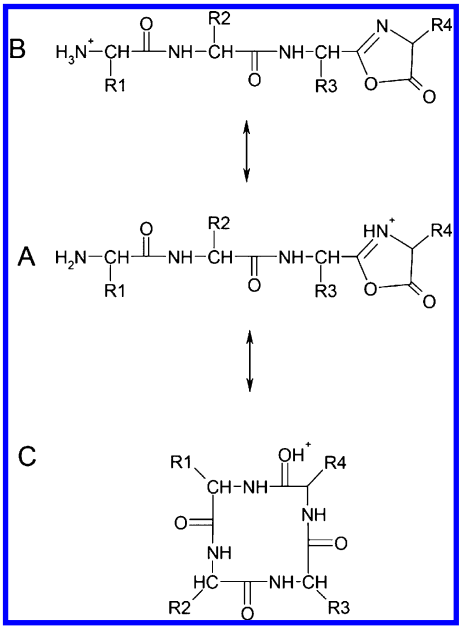

Information) are taken from ref 37, whereas the corresponding C structures (Figure S1, Supporting Information) were calculated in this work. For the b_4 ions with the AAAA sequence we calculated theoretical IR spectra for the structures (Figure 2) reported previously.[38] In the YGGF case we adapted the lowest energy linear and macrocyclic structures from previous potential energy surface scans.[6,7] It is to be noted that ref 7 discussed only structure C1, whereas structures C2 and C3 were not explicitly described in that work. The corresponding total and relative energies are given in Table S1 (Supporting Information). In the following we analyze the observed IR spectra with the help of theoretical spectra calculated for these representative structures. Because the experimental IR spectra observed for the GGGG and AAAA sequences are rather similar, only the latter will be discussed here in detail (calculated and experimental IR spectra of the b_4 ion of protonated GGGGG are provided in the Supporting Information in Figure S1).

The experimental IR spectrum of the AAAA b_4 ion is compared to the theoretical IR absorption spectra calculated for the lowest energy A, B, and C structures (Scheme 1) in Figure 2. A description of the vibrational modes of the three isomers is given in Table 1 where the scaled calculated wavenumbers and corresponding intensities are listed, along with the experimental positions of the bands. For each protonation site, the flexibility of the backbone allows for efficient charge solvation through intramolecular hydrogen bonding. The positively charged X$^+$–H (X = N, O) group forms a strong hydrogen bond with carbonyl groups. As a result, the band associated with the X$^+$–H stretch is strongly red-shifted and predicted to lie between 2500 and 3000 cm^{-1}. As found for protonated peptides[26−28,39] and various proton bound dimers,[40] this red shift is systematically accompanied by broadening of this band.

Broad infrared bands observed in the lower energy part of the IR spectra of the b_4 ions could thus be assigned to strongly hydrogen bonded X$^+$–H stretches. A few additional factors should be considered here. First, due to strong anharmonicity,

dx.doi.org/10.1021/jp400634t | J. Phys. Chem. A 2013, 117, 2508−2516

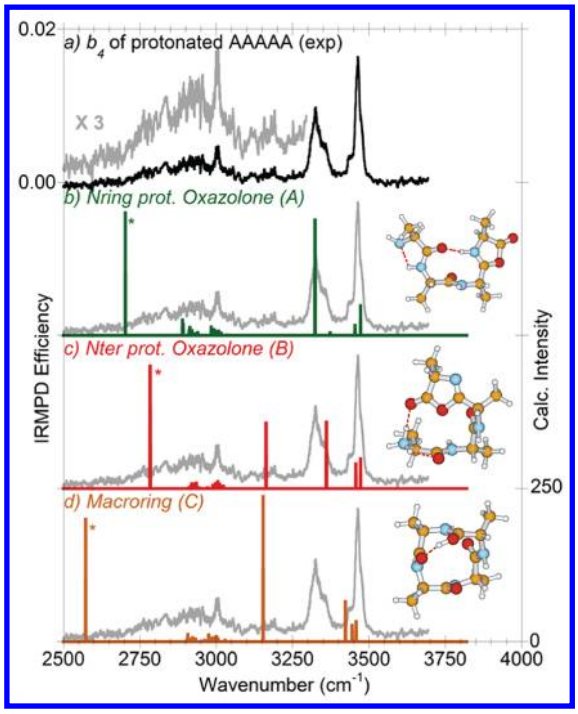

Figure 2. Experimental (a) and calculated (b–d) infrared spectra of the b_4 ion of protonated AAAAA. Theoretical spectra are presented for the ring-protonated oxazolone (A), the N-terminally protonated oxazolone (B), and the macrocyclic (C) isomers. A scaling factor value of 0.955 was used. The ZPE-corrected relative energies computed at the B3LYP/6-31+G(d,p) level are 0.0, 0.7, and 2.5 kcal mol^{-1} for the A, B, and C structures, respectively. To make the figure clearer, the stick-bars (marked with an asterisk) associated with large intensities (2140, 1176, 959 km·mol^{-1}, respectively) were truncated.

theoretical prediction of the frequencies of hydrogen bonded stretches is challenging[40] and no perfect match between experimental and harmonic theoretical frequencies should be expected. This phenomenon has been described in detail for proton bounded dimers.[40] The X^+–H frequency position strongly depends on the difference in proton affinity (PA) of the two basic sites sharing the proton,[40] and the potential energy surface along the proton motion is strongly anharmonic when the PA difference is small. In a recent spectroscopic report on protonated glycine and sarcosine containing dipeptides,[39] for example, it has been shown that the hydrogen to methyl substitution on the amino group has a dramatic effect on the experimental spectrum which is not predicted by theory using the harmonic approximation.

In addition, the situation is further complicated by the partial overlap with CH stretching bands. The sharp band observed at ~3007 cm^{-1} for the AAAA b_4 could be assigned to the nearly degenerate methyl asymmetric stretching modes of the alanine side chains, which are predicted between 3000 and 3050 cm^{-1} theoretically. One should notice that moderately IR active methyl symmetric CH and C_αH stretching modes are also predicted in the 2910–2940 cm^{-1} spectral range, i.e., near the maximum of the observed broad band.

The most structurally diagnostic part of the experimental spectrum ranges from 3100 to 3500 cm^{-1} where the A–C structures are predicted to have very different IR absorption bands. A visual inspection of the spectra displayed in Figure 2 indicates that the ring-protonated oxazolone isomer (A), which was found to be the lowest energy species on the potential energy surface (PES) of the AAAA b_4 ion, gives the best match for the spectral assignment. For each b_4 ion studied here, the lowest energy conformer of the N-ring protonated oxazolone structure is characterized by a very similar hydrogen bonding network. There is a strong ionic hydrogen bond formed between the N_{oxa}^+–H group and the amide CO of the first residue. The corresponding amide NH is in turn involved in a hydrogen bond with the terminal NH_2 group. This hydrogen bonding network is displayed in Scheme 2a where one can

Scheme 2. Hydrogen Bond Donor–Acceptor Motifs Found for the Lowest Energy Structures of (a) Protonated N_{ring} Oxazolone Isomers, and (b) Protonated Macrocyclic Isomers of b_4 Fragment Ions

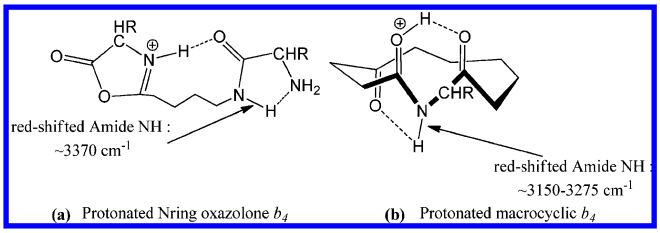

Table 1. Vibrational Modes of the b_4 Fragment of Protonated AAAAA[a]

experiment	N_{ring} oxa (A)	mode description	N_{ter} oxa (B)	mode description	macrocycle (C)	mode description
	2703 (2140)	s HB (H_2N^+H---O=C) NH	2784 (1176)	s HB (H_2N^+H---O=C) NH	2573 (959)	s HB (C=O$^+$H---O=C) OH
	2890–2940 (2/25)	CH_3 s-str and C_α-H	2911–2972 (1/8)	CH_3 s-str and C_α-H	2907–2983 (0/12)	CH_3 s-str and C_α-H
3302	2984–3037 (1/14)	CH_3 as-str	2989–3024 (3/8)	CH_3 as-str	2988–3030 (1/8)	CH_3 as-str
			3163 (107)	w HB (H_2N^+H--O=C) NH	3154 (237)	w HB (–C(O$^+$H)–N–H) NH[c]
3322	3323 (188)	w HB ($-H_2N$---HN) NH[b]				
shoulder	3373 (4)	NH_2 NH s-str	3362 (108)	free NH_3^+ NH		
					3423 (65)	amide NH
					3445 (26)	amide NH
shoulder	3455 (16)	NH_2 NH as-str	3457 (40)	amide NH	3458 (33)	amide NH
3464	3473 (48)	amide NH	3473 (49)	amide NH		

[a]Experimental and theoretical (scaling factor value: 0.955) wavenumbers are given in cm^{-1}; calculated intensities (in parentheses) are given in km·mol^{-1}; weak and strong hydrogen bonded OH or NH are indicated as "w HB" and "s HB", respectively. [b]Scheme 2a. [c]Scheme 2b.

dx.doi.org/10.1021/jp400634t | J. Phys. Chem. A 2013, 117, 2508–2516

notice that the N-terminal amide group forms a "hydrogen bond donor−acceptor" bridge. The corresponding N_{oxa}^{+}—H···O=C_{amide} and NH···NH_2− distances are ∼1.6 and ∼2.1 Å, respectively. The predicted IR spectrum of structure A reflects this hydrogen bonding pattern.

As discussed above, the frequency of the N_{oxa}^{+}−H stretching mode involved in a strong ionic hydrogen bond is strongly red-shifted (2703 cm^{-1}). The amide (Ala(2)) NH group involved in a weaker hydrogen bond is red-shifted to 3323 cm^{-1}, and the predicted intensity is large (Table 1) as compared to that of the second (free Ala(3)) amide NH (3473 cm^{-1}). As can be seen in Table 1, the predicted splitting between these two bands (150 cm^{-1}) is very close to the one (142 cm^{-1}) observed experimentally between the maxima of the two main IR bands (Figure 2a).

The asymmetric shape of the two experimental bands could be interpreted by considering the predicted positions of the symmetric (3373 cm^{-1}) and asymmetric (3455 cm^{-1}) NH_2 stretches of structure A (Figure 2b). The former would explain the blue shoulder of the band observed at ∼3322 cm^{-1}, and the latter the red-side shoulder of the band observed at ∼3464 cm^{-1}. It should be noted that the NH_2 asymmetric stretch, which is predicted at 3455 cm^{-1} in the present case, was found to provide a clear signature of the N-ring protonated structure of b_2 ions.[29,41] For larger b ions as the b_4 studied here, however, the limited resolution of our room temperature spectra prevents from a clear distinction of this mode with the free amide NH stretches.

The blue shoulder of the asymmetric band at ∼3322 cm^{-1} could also be interpreted as a signature of multiple conformers of N-ring protonated isomers or presence of conformers of N-terminal protonated oxazolone structures such as B (Figure 2c). The computed ZPE-corrected relative total and free energies of B at 0.7 and 1.6 kcal mol^{-1}, respectively, as compared to A indicate that both species can be present in our experiments. The terminal ammonium group in B is involved in a strong ionic hydrogen bond with the oxazolone CO group. This motif is characterized by a strongly red-shifted N^{+}—H mode (2784 cm^{-1} for structure B, Table 1). One of the two other ammonium NHs is also involved in a weaker hydrogen bond with the N terminal amide carbonyl and the corresponding N^{+}—H···O=C distance is ∼2.0−2.1 Å depending on the conformer. A very similar hydrogen bonding motif is also found for the lowest energy conformer of the N-terminal amino protonated oxazolone structure of the two other b_4 ions studied here. In the case of structure B (Figure 2c), the free and weakly hydrogen bonded ammonium NH stretches are predicted at 3362 and 3163 cm^{-1}, respectively, with similar intensities (∼100 km/mol, Table 1). The blue shoulder of the asymmetric band at ∼3322 cm^{-1} could thus be interpreted as a signature of a minor population of N-terminal protonated oxazolone structures such as B. As can be seen in Figure 2c, the two amide NH groups of this B structure are nearly free, as reflected by the positions of their stretching mode (3457 and 3473 cm^{-1}), which are predicted to be very close to the broad band at ∼3464 cm^{-1}. Although a very weak signal can be discerned, no significant experimental band is observed near 3163 cm^{-1}, i.e., the position of the weakly red-shifted ammonium stretch. It can thus be concluded that if any of N-terminal protonated oxazolone structures such as B is formed under our experimental conditions, the corresponding population is low.

Finally, population of macrocyclic structures such as C (Figure 2d) can be excluded for the b_4 fragment of polyalanine. Three out of the four amide NHs are nearly free, as reflected by their predicted positions (∼3400−3460 cm^{-1}, Table 1). The fourth amide NH is involved in a hydrogen bonding network shown in Scheme 2b. A very similar hydrogen bonding motif is found for the lowest energy conformers of protonated macrocyclic structures of the two other b_4 investigated here. Interestingly, as shown in Scheme 2b, the most favorable hydrogen bonding motif seems to be driven by the protonation site: the hydrogen bonded amide NH is the one of the protonated amide group. The predicted position of the red-shifted amide NH is 3154 cm^{-1} and the corresponding intensity is large (237 km·mol^{-1} for structure B, Table 1). An inspection of predicted IR absorption spectra of all the macrocyclic isomers (i.e., also higher energy isomers not shown in Figure 2) reveals that they all have a characteristic IR band in the 3150−3275 cm^{-1} spectral range. Because no experimental band is observed near 3150−3275 cm^{-1}, one can thus safely conclude that macrocyclic structures of the AAAA b_4 ions are not present in large amounts under our experimental conditions.

As discussed above, the IR spectra of the b_4 ions of protonated GGGGG and AAAAA are very similar to each other (Figure 1). The experimental IR spectrum of the GGGG b_4 is compared to theoretical spectra computed for the three main structure types (A−C, Scheme 1) in Figure S1 (Supporting Information; see also Table S2 in the Supporting Information for a detailed description of the vibrational modes). In the low-energy part of the GGGG spectrum, a broad yet structured band is observed even if its intensity is lower than that observed for the AAAA b_4 ion. Similarly to the AAAA case, it is impossible to propose a definitive assignment from this part of the IR spectrum. The 3100−3500 cm^{-1} range of the experimental IR spectrum is more informative and similarly to the AAAA case the GGGG spectrum is dominated by two bands. The predicted spectra for the three types of structures are also very similar for the two cases (Figures 2b,c and S1b,c, Supporting Information). One can thus safely conclude that macrocyclic structures are not formed in the case of the GGGG b_4 ion. Similarly to the AAAA case, it would be conceivable that the b_4 ions of protonated G_5 are formed as a mixture of N_{ring} (A) and N_{ter} (B) protonated oxazolone structures. Nevertheless, the fact that no band is observed experimentally near ∼3100 cm^{-1}, where an intense ammonium stretch is predicted for B, suggests that the population of the N_{ter} protonated structure is small. Similarly to the AAAA b_4 case, the A structure is energetically more favored than B (ΔE_{ZPE} at 1.9 kcal mol^{-1} and ΔG at 2.9 kcal mol^{-1}) or C (ΔE_{ZPE} at 3.5 kcal mol^{-1} and ΔG at 6.5 kcal mol^{-1}), in agreement with the experimental data.

Figure 3 compares the experimental IR spectrum of the b_4 ion of protonated YGGFL to the calculated IR spectra of the lowest energy A and B structures[6,7] (Figure 3b,c, respectively) and three low-energy cyclo-(YGGF) structures.[6,7] Three macrocyclic structures are considered, with the ionizing proton at the amide oxygens of the Y−F, G−G, and G−F amide bonds, respectively (named C1, C2, and C3 in Figures 3d−f, respectively). The experimental positions of the IRMPD bands are given in Table 2, along with the predicted frequencies and corresponding intensities of each of the five structures considered in Figure 3. The IR spectrum of the b_4 ion of protonated YGGFL (Figure 1c) is more structured than those of the GGGG and AAAA b_4 ions (Figure 1a,b, respectively), which could reasonably be assigned on the basis of the linear, C-terminal protonated oxazolone structures.

dx.doi.org/10.1021/jp400634t | J. Phys. Chem. A 2013, 117, 2508−2516

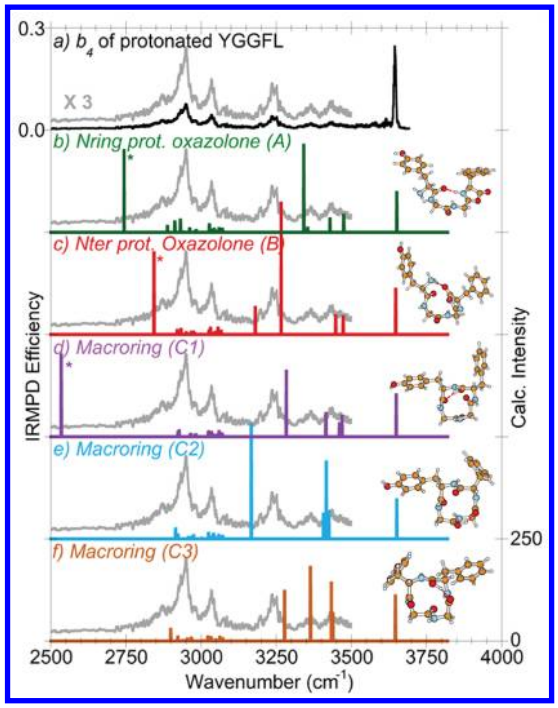

Figure 3. Experimental (a) and calculated (b–f) infrared spectra of the b_4 ion of protonated YGGFL. Theoretical spectra are presented for the ring-protonated oxazolone (A), the N-terminally protonated oxazolone (B), and macrocyclic isomers protonated at the Tyr-Phe (C1), Gly-Gly (C2), and Gly-Phe (C3) amide oxygens. A scaling factor value of 0.955 was used. The ZPE-corrected relative energies computed at the B3LYP/6-31+G(d,p) level are 0.0, −1.6, +2.1, +3.2, and +2.0 kcal mol^{-1} for the A, B, C1, C2, and C3 structures, respectively. To make the figure clearer, the stick-bars (marked with an asterisk) associated with large intensities (2246, 1543, 1208, 1013, 904 km·mol^{-1}, respectively) were truncated.

The very same YGGF b_4 ion has recently been investigated using the IR/UV double resonance technique performed in a cryogenically cooled ion trap where the temperature is estimated to be ∼10 K.[27] The IR/UV technique provides higher resolution than our experimental setup. Additionally, isomer selection is possible due to the double resonance strategy applied and four isomers of the YGGF b_4 ion were reported. Spectral assignment was supported by nitrogen-15 isotopic substitution of individual amino acids and assisted by density functional theory calculations. For all four isomers, two amide NH bands were observed, which suggested that they had an oxazolone structure. Furthermore, the absence of spectral shifts associated with ^{15}N substitution on the F residue and of a band near 3450 cm^{-1} (i.e., symmetric NH_2 stretch) led to the conclusion that the four observed IR/UV spectra can be assigned to four conformers of N-terminal protonated oxazolone isomers. IR/UV spectra recorded in the fingerprint region supported these structural assignments. It is to be noted that despite extensive sampling of the potential energy surface, no satisfactory match between computed structures and the four experimental spectra could be obtained. This was especially true for the 2700–3200 cm^{-1} range that is most likely dominated by NH_3^+ stretches whereas theory most likely overestimates the NH_2^+—H···O=C hydrogen bond strength and this causes overestimated red shifts of the NH and C=O stretches.[27]

Table 2. Vibrational Modes of the b_4 Fragment of Protonated YGGFL[a]

experiment	macrocycle (C3)	macrocycle (C2)	macrocycle (C1)	mode description	N_{ter} oxa (B)	mode description	N_{ring} oxa (A)	mode description
	2619 (997)	2496 (1013)	2535 (1208)	s HB (C=O$^+$H···O=C) OH	2844 (1543)	s HB (H_2N^+H···O=C) NH	2744 (2246)	s HB (H_2N^+H···O=C) NH
2945	2899–3038 (0/29)	2915–3039 (0/24)	2899–3038 (0/29)	aliphatic CH	2920–3027 (1/12)	aliphatic CH	2889–2984 (1/22)	aliphatic CH
3035	3022–3073 (0/10)	3025–3072 (0/13)	3022–3073 (0/10)	aromatic CH	3027–3076 (0/16)	aromatic CH	3028–3071 (2/19)	aromatic CH
					3181 (66)	w HB (H_2N^+H···O=C) NH		
3238	3278 (122)	3168 (279)	3284 (160)	w HB (−C(O$^+$H)–N–H) NH[c]	3267 (321)	w HB (H_2N^+H···Tyr) NH		
							3342 (213)	w HB (−H_2N···H–N) NH[b]
3365	3364 (180)			amide NH			3355 (10)	s −NH_2 NH
		3407 (60)	3416 (56)		3448 (45)	amide NH	3429 (33)	as −NH_2 NH
3433	3434 (142)	3416 (188)	3461 (31)	amide NH	3472 (43)	amide NH	3475 (42)	amide NH
	3438 (67)	3426 (65)	3469 (50)	amide NH				
3644	3647 (110)	3651 (96)	3649 (102)	Tyr OH	3647 (111)	Tyr OH	3652 (98)	Tyr OH

[a]Experimental and theoretical (scaling factor value: 0.955) wavenumbers are given in cm^{-1}; calculated intensities (in parentheses) are given in km.mol^{-1}; weak and strong hydrogen bonded OH or NH are indicated as "w HB" and "s HB", respectively;. [b]Scheme 2a. [c]Scheme 2b.

dx.doi.org/10.1021/jp400634t | J. Phys. Chem. A 2013, 117, 2508–2516

These DFT deficiencies should be kept in mind whereas attempting assignment of our room temperature spectrum of the b_4 ion of protonated YGGFL. As compared to the isomer-specific IR/UV spectra discussed above, IR bands are broader in the present case. Furthermore, the population of multiple conformers and possibly of multiple isomers may further complicate the room temperature IR spectra of mass-selected ions. The spectral assignment is more challenging than for the GGGG and AAAA b_4 fragments, and no unambiguous spectral assignment can be given on the basis of the PES data available in the literature.[6,7] That is, none of the calculated IR absorption spectra perfectly matches all experimental bands, especially those in the 3100−3500 cm^{-1} range. Yet, two distinct assignments of our room temperature spectrum can be proposed on the basis of the available experimental and theoretical information.

Comparison of the present and the UV/IR spectra of ref 27 suggests that our room temperature ion population is also dominated by N-terminal protonated oxazolone isomers (B, Figure 3c). The frequency splitting between the two amide NH bands was reported[27] to vary from 17 to 59 cm^{-1} depending on the isomer observed (A, 3430 and 3461 cm^{-1}; B, 3348 and 3407 cm^{-1}; C, 3446 and 3469 cm^{-1}; D, 3417 and 3434 cm^{-1}; nomenclature of ref 27 is used here). In the present case, the two bands with maxima at 3365 and 3433 cm^{-1} could be assigned to the two amide NH stretches (Table 2). The positions of these bands are similar to those observed for isomer B of ref 27, which also had a band centered at 3222 cm^{-1}, which was assigned to an ammonium stretch. Interestingly, a band is observed at a similar position (3238 cm^{-1}) in our case. Two other bands observed at 2900 and 3082 cm^{-1} for isomer C in ref 27 were assigned to the two other ammonium stretches. In the present case, the bands with maxima at 2945 and 3035 could also be assigned to these ammonium stretches. As a result, our room temperature IR spectrum is compatible with the formation of N-terminal protonated oxazolone structures. However, the theoretical spectrum computed for structure B (Figure 3c) does not perfectly match with the experimental spectrum. As already noted in ref 27, this is especially true in the low-energy part of the spectrum where the ammonium NH stretches are expected. Considering the conformational flexibility of the system and the difficulty to describe its hydrogen bonding network, it is better to consider theoretical structures only as a guide for spectral assignment.

The alternative interpretation indicates that macrocyclic structures such as C3 (Figure 3f) are present under our experimental conditions. Altough structure B is energetically more favored than any of the C structures (Table S2, Supporting Information), our computational strategy based on the harmonic approximation to compute vibrational frequencies is most likely overestimating entropy effects for the latter. As can be seen in Table 2, the three macrocyclic structures are predicted to have a quite intense (120−280 $km{\cdot}mol^{-1}$) absorption band between ∼3150 and ∼3300 cm^{-1}. The corresponding normal mode involves the stretching of a hydrogen bonded amide NH as depicted in Scheme 2b. In the case of the macrocyclic structure C3, this band is predicted at 3278 cm^{-1}, i.e., close to the position (3238 cm^{-1}) of an experimental band. Assuming that structure C3 is formed under our experimental conditions, a spectral assignment could be proposed (Table 2). The C3 structure has two free amide NH with a stretching frequency predicted at 3434 and 3438 cm^{-1}, the former being more intense, which could explain the observation of one band at ∼3433 cm^{-1}. Structure C3 has a band predicted at 3364 cm^{-1}, very close to the position of an experimental band (∼3365 cm^{-1}). It corresponds to the stretching mode of an NH group pointing toward the tyrosine aromatic ring, which explains the slight red shift.

An inspection of Table 2 reveals that the OH stretch associated with the strong hydrogen bond between the protonated carbonyl and an adjacent carbonyl group is predicted to be strongly red-shifted (between 2496 and 2619 cm^{-1}, depending on the macrocyclic structure, Table 2). As discussed above, the theoretical description of such a proton shift between two basic sites is difficult, and the presently used harmonic approximation is not expected to accurately predict the corresponding frequency. One could thus tentatively assign the broad feature extending from 2750 to 3000 cm^{-1} to the red-shifted C═O$^+$—H stretch. Finally, the two sharp bands that emerge from this broad band, with maxima near ∼2950 and ∼3040 cm^{-1} nicely match with IR absorption bands common in all A-Cn structures. The band at ∼2950 cm^{-1} can be assigned as the asymmetric CH stretch of the methylene group of the tyrosine and phenylalanine residues, which are predicted at 2924 and 2928 cm^{-1}. The band at ∼3040 cm^{-1} can be assigned to aromatic CH stretches of the phenylalanine and tyrosine residues, which are predicted at ∼3020−3030 cm^{-1}. The observation of quite intense IRMPD bands on resonance with relatively weakly IR active CH stretching modes may sound surprising. It should be noted, however, that the near degeneracy of several CH stretching modes is likely to facilitate the multiple photon absorption process, ultimately leading to the fragmentation of the precursor ions, as observed in other cases.[30]

CONCLUSION

Room temperature IR spectra of b_4 fragments of protonated G_5, Ala_5, and YGGFL are presented here. This study provides a complement to the recent double resonance IR/UV study of the b_4 ion of YGGFL trapped in a cryogenically cooled (∼10 K) ion trap.[27] With this latter high-resolution approach, isomer selective high-resolution IR spectroscopy can be achieved, but it is limited to UV-chromophore containing systems. Extension to the cases of b_4 fragments of protonated G_5 and Ala_5 shows that the two corresponding spectra are rather similar. However, they are clearly different from that of the b_4 fragment ion of protonated YGGFL. As proposed in ref 27, the YGGF b_4 IR spectrum can be assigned to the N_{ter} protonated oxazolone structure. Nevertheless, as already pointed out in ref 27, no perfect match can be found with the predicted IR absorption spectrum of a single conformer of this structure. This is especially true in the low-energy part of the IR spectrum where the characteristic ammonium NH stretches are expected. This observation points to the general difficulty for describing the energetics of potential energy surfaces when strong hydrogen bonding is involved. It should be noted, however, that it could also reveal some problems with the study of large and flexible biomolecules cooled at low temperature because multiple, not necessarily low-energy conformers may be populated during the fast cooling process.

An alternative interpretation of the IR spectrum of the YGGF b_4 fragment is proposed here. It is shown that all low-energy conformers of b_4 macrocyclic structures are predicted to have a hydrogen bond network where an amide group, protonated on its carbonyl, acts as a hydrogen bond donor−acceptor group

and is characterized by a moderately red-shifted NH. Overall, it is shown that the predicted IR spectrum of a macrocyclic structure reasonably matches with the experimental spectrum. We are in a process to extend this work to other including larger b_n fragment ions for which cyclic peptides can be used as reference to determine clear-cut IR signature of macrocyclic structures. IR spectroscopy of isolated gas-phase ions provide a useful guide for theory because the characterization of the IR spectrum of hydrogen bonded biopolymers remains a challenge due to the strong anharmonicity. We are currently experimenting with computational strategies which go beyond the harmonic approximation in calculating theoretical IR spectra.

■ ASSOCIATED CONTENT

Supporting Information

IR spectra of the b_4 ion of protonated GGGGG (Figure S1). Energetics of the b_4 ion of protonated YGGFL (Table S1). Vibrational assignment of the b_4 ion of protonated GGGGG (Table S2). Complete ref 36. This material is available free of charge via the Internet at http://pubs.acs.org.

■ AUTHOR INFORMATION

Corresponding Author

*E-mail: B.Paizs@dkfz.de, Philippe.Maitre@u-psud.fr.

Notes

The authors declare no competing financial interest.

■ ACKNOWLEDGMENTS

B.P. thanks the Deutsche Forschungsgemeinschaft for a Heisenberg fellowship. Financial support by the European Commission (seventh framework programme, grant number 226716) is gratefully acknowledged. M.R. thanks the CONICET (Argentina) and the MESR (France) for a postdoctoral fellowship. The authors are grateful to V. Steinmetz for technical support. Financial support from the TGE FT-ICR for conducting the research is gratefully acknowledged.

■ ADDITIONAL NOTE

Originally submitted for the "Peter B. Armentrout Festschrift", published as the February 14, 2013, issue of *J. Phys. Chem. A* (Vol. 117, No. 6).

■ REFERENCES

(1) Steen, H.; Mann, M. The abc's (and xyz's) of Peptide Sequencing. *Nat. Rev. Mol. Cell. Biol.* **2004**, *5*, 699−711.

(2) Roepstorff, P.; Fohlmann, J. J. Proposals for a Common Nomenclature for Sequence Ions in Mass Spectra of Peptides. *Biomed. Mass Spectrom.* **1984**, *11*, 601−601.

(3) Biemann, K. Contributions of Mass Spectrometry to Peptide and Protein Structure. *Biomed. Environ. Mass Spectrom.* **1988**, *16*, 99−111.

(4) Nesvizhskii, A. E.; Vitek, O.; Aebersold, R. Analysis and Validation of Proteomic Data Generated by Tandem Mass Spectrometry. *Nat. Methods* **2007**, *4*, 787−797.

(5) Paizs, B.; Suhai, S. Fragmentation Pathways of Protonated Peptides. *Mass Spectrom. Rev.* **2005**, *24*, 508−548.

(6) Polfer, N. C.; Oomens, J.; Suhai, S.; Paizs, B. Spectroscopic and Theoretical Evidence for Oxazolone Ring Formation in Collision-Induced Dissociation of Peptides. *J. Am. Chem. Soc.* **2005**, *127*, 17154−17155.

(7) Polfer, N. C.; Oomens, J.; Suhai, S.; Paizs, B. Infrared Spectroscopy and Theoretical Studies on Gas-Phase Protonated Leu-Enkephalin and Its Fragments: Direct Experimental Evidence for the Mobile Proton. *J. Am. Chem. Soc.* **2007**, *129*, 5887−5897.

(8) Yoon, S. H.; Chamot-Rooke, J.; Perkins, B. R.; Hilderbrand, A. E.; Poutsma, J. C.; Wysocki, V. H. IRMPD Spectroscopy Shows That AGG Forms an Oxazolone b_2^+ Ion. *J. Am. Chem. Soc.* **2008**, *130*, 17644−17645.

(9) Bythell, B. J.; Erlekam, U.; Paizs, B.; Maitre, P. Infrared Spectroscopy of Fragments Derived from Tryptic Peptides. *ChemPhysChem* **2009**, *10*, 883−885.

(10) Erlekam, U.; Bythell, B. J.; Scuderi, D.; Van Stipdonk, M.; Paizs, B.; Maitre, P. Infrared Spectroscopy of Fragments of Protonated Peptides. Direct Evidence for Macrocyclic Structure of b_5 Ions. *J. Am. Chem. Soc.* **2009**, *131*, 11503−11508.

(11) Verkerk, U. H.; Siu, C. K.; Steill, J. D.; El Aribi, H.; Zhao, J. F.; Rodriquez, C. F.; Oomens, J.; Hopkinson, A. C.; Siu, K. W. M. a_2 Ion Derived from Triglycine: An N_1-Protonated 4-Imidazolidinone. *J. Phys. Chem. Lett.* **2010**, *1*, 868−872.

(12) Bythell, B. J.; Maître, P.; Paizs, B. Cyclization and Rearrangement Reactions of a_n Fragment Ions of Protonated Peptides. *J. Am. Chem. Soc.* **2010**, *132*, 14766−14779.

(13) Oomens, J.; Young, S.; Molesworth, S.; van Stipdonk, M. Spectroscopic Evidence for an Oxazolone Structure of the b_2 Fragment Ion from Protonated Tri-Alanine. *J. Am. Soc. Mass Spectrom.* **2009**, *20*, 334−339.

(14) Prazeres, R.; Glotin, F.; Insa, C.; Jaroszynski, D. A.; Ortega, J. M. Two-Colour Operation of a Free-Electron Laser and Applications in the Mid-Infrared. *Eur. Phys. J. D* **1998**, *3*, 87−93.

(15) Oepts, D.; Van der Meer, A. F. G.; Van Amersfoort, P. W. The Free-Electron-Laser User Facility Felix. *Infrared Phys. Technol.* **1995**, *36*, 297−308.

(16) Yalcin, T.; Khouw, C.; Csizmadia, I. G.; Peterson, M. R.; Harrison, A. G. Why Are *b* Ions Stable Species in Peptide Mass Spectra? *J. Am. Soc. Mass Spectrom.* **1995**, *6*, 1165−1174.

(17) Yalcin, T.; Csizmadia, I. G.; Peterson, M. R.; Harrison, A. G. The Structure and Fragmentation of B_n ($n \geq 3$) Ions in Peptide Spectra. *J. Am. Soc. Mass Spectrom.* **1996**, *7*, 233−242.

(18) Perkins, B.; Chamot-Rooke, J.; Yoon, S.; Gucinski, A.; Somogyi, A.; Wysocki, V. H. Evidence of Diketopiperazine and Oxazolone Structures for HA b_2^+ Ion. *J. Am. Chem. Soc.* **2009**, *131*, 17528−17529.

(19) Harrison, A. G.; Young, A. B.; Bleiholder, C.; Suhai, S.; Paizs, B. Scrambling of Sequence Information in Collision-Induced Dissociation of Peptides. *J. Am. Chem. Soc.* **2006**, *128*, 10364−10365.

(20) Bleiholder, C.; Osburn, S.; Williams, T. D.; Suhai, S.; Van Stipdonk, M.; Harrison, A. G.; Paizs, B. Sequence-Scrambling Pathways of Protonated Peptides. *J. Am. Chem. Soc.* **2008**, *130*, 17774−17789.

(21) Snoek, L. C.; Robertson, E. G.; Kroemer, R. T.; Simons, J. P. Conformational Landscapes in Amino Acids: Infrared and Ultraviolet Ion-Dip Spectroscopy of Phenylalanine in the Gas Phase. *Chem. Phys. Lett.* **2000**, *321*, 49−56.

(22) Robertson, E. G.; Simons, J. P. Getting into Shape: Conformational and Supramolecular Landscapes in Small Biomolecules and Their Hydrated Clusters. *Phys. Chem. Chem. Phys.* **2001**, *3*, 1−18.

(23) Gerhards, M.; Unterberg, C. Structures of the Protected Amino Acid Ac-Phe-OMe and its dimer: A β-sheet Model System in the Gas Phase. *Phys. Chem. Chem. Phys.* **2002**, *4*, 1760−1765.

(24) Unterberg, C.; Gerlach, A.; Schrader, T.; Gerhards, M. Structure of the Protected Dipeptide Ac-Val-Phe-OMe in the Gas Phase: Towards a β-sheet Model System. *J. Chem. Phys.* **2003**, *118*, 8296−8300.

(25) Mons, M.; Dimicoli, I.; Tardivel, B.; Piuzzi, F.; Robertson, E. G.; Simons, J. P. Energetics of the Gas Phase Hydrates of Trans-Formanilide: A Microscopic Approach to the Hydration Sites of the Peptide Bond. *J. Phys. Chem. A* **2001**, *105*, 969−973.

(26) Nagornova, N. S.; Guglielmi, M.; Doemer, M.; Tavernelli, I.; Rothlisberger, U.; Rizzo, T. R.; Boyarkin, O. V. Cold-Ion Spectroscopy Reveals the Intrinsic Structure of a Decapeptide. *Angew. Chem., Int. Ed.* **2011**, *50*, 5383−5386.

(27) Wassermann, T. N.; Boyarkin, O. V.; Paizs, B.; Rizzo, T. R. Conformation-Specific Spectroscopy of Peptide Fragment Ions in a

Low-Temperature Ion Trap. *J. Am. Soc. Mass Spectrom.* **2012**, *23*, 1029−1045.
(28) Kamrath, M. Z.; Garand, E.; Jordan, P. A.; Leavitt, C. M.; Wolk, A. B.; Van Stipdonk, M. J.; Miller, S. J.; Johnson, M. A. Vibrational Characterization of Simple Peptides Using Cryogenic Infrared Photodissociation of H_2-Tagged, Mass-Selected Ions. *J. Am. Chem. Soc.* **2011**, *133*, 6440−6448.
(29) Sinha, R. K.; Erlekam, U.; Bythell, B. J.; Paizs, B.; Maître, P. Diagnosing the Protonation Site of b_2 Peptide Fragment Ions Using IRMPD in the X−H (X = O, N, and C) Stretching Region. *J. Am. Soc. Mass Spectrom.* **2011**, *22*, 1645−1650.
(30) Bakker, J. M.; Besson, T.; Lemaire, J.; Scuderi, D.; Maitre, P. Gas-Phase Structure of a π-Allyl-Palladium Complex: Efficient Infrared Spectroscopy in a 7 T Fourier Transform Mass Spectrometer. *J. Phys. Chem. A* **2007**, *111*, 13415−13424.
(31) Bakker, J. M.; Sinha, R. K.; Besson, T.; Brugnara, M.; Tosi, P.; Salpin, J. Y.; Maitre, P. Tautomerism of Uracil Probed via Infrared Spectroscopy of Singly Hydrated Protonated Uracil. *J. Phys. Chem. A* **2008**, *112*, 12393−12400.
(32) Sinha, R. K.; Nicol, E.; Steinmetz, V.; Maitre, P. Gas Phase Structure of Micro-Hydrated $[Mn(ClO_4)]^+$ and $[Mn_2(ClO_4)_3]^+$ Ions Probed by Infrared Spectroscopy. *J. Am. Soc. Mass Spectrom.* **2010**, *21*, 758−772.
(33) Yeh, L. I.; Okumura, M.; Myers, J. D.; Price, J. M.; Lee, Y. T. Vibrational Spectroscopy of the Hydrated Hydronium Cluster Ions $H_3O^+\cdot(H_2O)_n$ (n = 1, 2, 3). *J. Chem. Phys.* **1989**, *91*, 7319−7330.
(34) Peiris, D. M.; Cheeseman, M. A.; Ramanathan, R.; Eyler, J. R. Infrared Multiple Photon Dissociation Spectra of Gaseous Ions. *J. Phys. Chem.* **1993**, *97*, 7839−7843.
(35) Guidi, M.; Lorenz, U. J.; Papadopoulos, G.; Boyarkin, O. V.; Rizzo, T. R. Spectroscopy of Protonated Peptides Assisted by Infrared Multiple Photon Excitation. *J. Phys. Chem. A* **2009**, *113*, 797−799.
(36) Frisch, M. J.; Trucks, G. W.; Schlegel, H. B.; Scuseria, G. E.; Robb, M. A.; Cheeseman, J. R.; Montgomery, J. A.; Vreven, Jr.,T.; Kudin, K. N.; Burant, J. C.; et al. *Gaussian 03*, Revision C.02; Gaussian, Inc.: Wallingford, CT, 2004. See Supporting Information for full reference.
(37) Bythell, B. J.; Dain, R. P.; Curtice, S. S.; Oomens, J.; Steill, J. D.; Groenewold, G. S.; Paizs, B.; Van Stipdonk, M. The Structure of $[M+H\text{-}H_2O]^+$ from Protonated Tetraglcine Revealed by Tandem Mass Spectrometry and IRMPD Spectroscopy. *J. Phys. Chem. A* **2010**, *114*, 5076−5082.
(38) Allen, J. M.; Racine, A. H.; Berman, A. M.; Johnson, J. S.; Bythell, B. J.; Paizs, B.; Glish, G. L. Why Are a_3 Ions Rarely Observed? *J. Am. Soc. Mass Spectrom.* **2008**, *19*, 1764−1770.
(39) Leavitt, C. M.; Wolk, A. B.; Kamrath, M. Z.; Garand, E.; van Stipdonk, J.; Johnson, M. A. Characterizing the Intramolecular H-bond and Secondary Structure in Methylated $GlyGlyH^+$ with H_2 Predissociation Spectroscopy. *J. Am. Soc. Mass Spectrom.* **2011**, *22*, 1941−1952.
(40) Roscioli, J. R.; McCunn, L. R.; Johnson, M. A. Quantum Structure of the Intermolecular Proton Bond. *Science* **2007**, *316*, 249−254.
(41) Wang, D.; Gulyuz, K.; Stedwell, C. N.; Polfer, N. C. Diagnostic NH and OH Vibrations for Oxazolone and Diketopiperazine Structures: b_2 from Protonated Triglycine. *J. Am. Soc. Mass Spectrom.* **2011**, *22*, 1197−1203.